

A mapping approach to synchronization in the "Zajfman trap": stability conditions and the synchronization mechanism

Tihamér Geyer and David J Tannor

Department of Chemical Physics, Weizmann Institute of Science, Rehovot 76100, Israel

We present a two particle model to explain the mechanism that stabilizes a bunch of positively charged ions in an "ion trap resonator" [Pedersen *etal*, *Phys. Rev. Lett.* **87** (2001) 055001]. The model decomposes the motion of the two ions into two mappings for the free motion in different parts of the trap and one for a compressing momentum kick. The ions' interaction is modelled by a time delay, which then changes the balance between adjacent momentum kicks. Through these mappings we identify the microscopic process that is responsible for synchronization and give the conditions for that regime.

PACS numbers: 39.10.+j, 45.50.-j

I. INTRODUCTION

Ion traps are widely used to store ions for long periods to obtain high resolution spectroscopy. Ions of the same charge repel each other through their long range Coulomb potential, so the trap has the purpose of localizing the ions in the measurement region. Recently a quite surprising behavior was discovered [1], where, under special conditions, ions in an ion trap resonator do not diffuse into the whole trap but stay together as a bunch for arbitrarily long times. This synchronized, collective motion occurs only for certain parameters of the trap fields, but in these regions it is stable.

This observation, which is puzzling and of intriguing scientific interest in its own right, has important technological applications. Pedersen *etal* have suggested the use of the small "table top" ion trap as a time-of-flight mass spectrometer. As the observation time, and therefore the effective length of the spectrometer, are in principle only limited by collisions between the ions, mass resolutions can be envisioned which are otherwise only achieved in storage rings [2]. Indeed, the high resolution spectroscopy suggested in [1] has now been achieved [3].

Until now this synchronization effect has not been fully understood; from the experimental observations [4, 5] it appears that the trap has to be operated in a regime where the ions' periods in the trap *increase* with their energy. Other tests point out that the focussing of the beam inside the mirrors is important. Numerical simulations confirm these empirical findings, but they, too, can not decide, if the requirements found so far, are complete and if they really stem from the underlying microscopic process.

A macroscopic explanation of the synchronization effect in terms of a "negative mass instability" was recently presented in [3]. It confirms that the ions' period has to increase with their energy and shows that a minimal density inside the bunch is necessary to support synchronization. But, being a mean field treatment, it can not give a detailed explanation of the underlying microscopic dynamics and it is insensitive to certain properties of the trapping field.

The aim of this paper is therefore, to set up a complementary microscopic model of the ions in the trap, which is simple enough to be understood completely. With this model we then can explain the basic mechanism, determine the necessary conditions for synchronization, check their completeness and finally understand how the size of the bunch depends on the parameters of the trap and those of the ion beam.

In this paper we concentrate on deriving the conditions for stability and we explain and illustrate the fundamental mechanism. The stability limits and the behavior of the macroscopic bunch will be presented in a following paper [6].

This paper is organized as follows: In section II we explain the model of the trap. In section III we lay out the framework of the dynamics in terms of the mappings for two non interacting ions. Then, in section IV, we explain how their interaction is incorporated in the mappings. With the interaction added we derive the conditions for bunching, section V, and explain the underlying mechanism in section VI. In section VII we confirm that the conditions and explanations given are in fact applicable to the experiment.

II. THE MODEL OF THE TRAP

The experimental setup and the observed behavior is described in great detail in [4, 5]. We will therefore only cite what we need to build up the model. In the experiment a bunch of ions is injected into the "ion trap resonator" and its width observed, when it passes through a ring shaped pickup electrode in the trap's center. When the field gradient in the electrostatic mirrors is below a certain threshold, the bunch does not diffuse.

Numerical simulations with many ions performed by Pedersen *etal* have shown synchronization in a one dimensional model [5]. We will consider a one dimensional model, too, and use the same simplified trap potential, which consists of the central field free region of length L and two slopes with a constant gradient F , the electrostatic mirrors. The two einzel lenses, which focus the

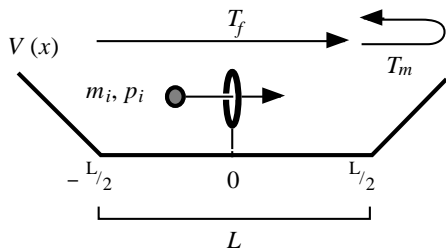


FIG. 1: Model of the trap: the simplified potential $V(x)$ (1) with the ions taking time T_f through the central part and T_m to return from the mirror. The ring shaped pickup electrode is located in the center of the trap.

beam into the mirrors [4], are neglected. They are only necessary for keeping the beam inside the trap. This setup is modelled by the potential

$$V(x) = \begin{cases} 0 & \text{when } |x| \leq \frac{L}{2} \\ (|x| - \frac{L}{2})F & \text{when } |x| > \frac{L}{2} \end{cases} \quad (1)$$

We will not treat the whole bunch, but will look at the behavior of only two identical ions in the trap and explain how these two ions synchronize their motion.

Since synchronization is a property of the relative coordinate, we describe these two ions in relative and center of mass (CM) coordinates:

$$\begin{aligned} M &= 2m & R &= \frac{x_1 + x_2}{2} & P &= p_1 + p_2 \\ \mu &= \frac{m}{2} & x &= x_1 - x_2 & p &= \frac{p_1 - p_2}{2} \end{aligned} \quad (2)$$

Capital letters denote CM properties and lowercase letters are used for the relative coordinate. With the ion-ion interaction $W(x)$ the Hamiltonian now reads:

$$H = \frac{P^2}{2M} + \frac{p^2}{2\mu} + qV(R + \frac{x}{2}) + qV(R - \frac{x}{2}) + q^2W(x) \quad (3)$$

Without loss of generality we set the charge of the ions to $q = +1$ in the following. Though $W(x)$ could be an arbitrary two body interaction we will think of it as the repulsive Coulomb potential between two positively charged ions.

Our model will not be exact. In order to check the validity of the various approximations which we perform, we insert the values from the original experiment, in which the bunching effect was observed initially [1]. These values are given in table I. If not otherwise stated we use atomic units in the following.

An ion with the momentum $p_0 = \sqrt{2mE_0}$ will spend time T_m in the mirror, which can also be expressed in terms of the CM momentum:

$$T_m = \frac{2p_0}{F} = \frac{P}{F} \quad (4)$$

Ions with a velocity $p_0/m = P/M$ need the time T_f to pass through the central field free region of the trap:

$$T_f = \frac{Lm}{p_0} = \frac{LM}{P} := \alpha T_m \quad (5)$$

quantity	value	in a.u.
length L	200 mm	$= 3.78 \times 10^9$ a.u.
mirror field gradient qF	$80 \frac{\text{keV}}{\text{m}}$	$= 1.56 \times 10^{-7} \frac{\text{a.u.}}{\text{a.u.}}$
ion mass m (Ar^+)	40 amu	$= 7.35 \times 10^4$ a.u.
ion energy E_0	4.2 keV	$= 154$ a.u.
ion momentum p_i		4.76×10^3 a.u.
beam radius d	10 μm	$= 1.89 \times 10^5$ a.u.
time in the mirror T_m	1.48 μs	$= 6.10 \times 10^{10}$ a.u.
time in the center T_f	1.41 μs	$= 5.84 \times 10^{10}$ a.u.
dispersion parameter α		0.956

TABLE I: Parameters and sizes used in our calculations. These values are the same as in the original experiment, in which bunching was originally discovered [1].

Here we have introduced the “dispersion parameter” $\alpha = \frac{LmF}{2p_0^2}$ as the ratio of the two times T_f and T_m . With these the total time T for the period of one ion becomes:

$$T = 2T_m + 2T_f = 2(1 + \alpha)T_m = \frac{4p_0}{F} + \frac{2Lm}{p_0} \quad (6)$$

From this equation we calculate the “dispersion” $\frac{\partial T}{\partial p_0}$ of the trap:

$$\frac{\partial T}{\partial p_0} = \frac{4}{F} - \frac{2Lm}{p_0^2} = \frac{4}{F}(1 - \alpha) \quad (7)$$

In the experiment and in the theoretical model of reference [3] the ions were found to synchronize, when the dispersion is positive, i.e, when an ion with a higher momentum (energy) takes longer to complete one period in the trap. With (5) we have $\alpha < 1$: the ions then spend more time in the mirror than in the central region.

Two ions with different momenta have different periods, which in turn can be reformulated as a difference Δx in their distance when we propagate both ions for the same time T . To calculate Δx , we linearize T (6) around the mean momentum $\frac{P}{2}$. With the difference in the ions’ momenta of $\Delta p = 2p$ (2) the difference between their periods is $\Delta T = \frac{\partial T}{\partial p_0} \Delta p$. During that interval the ions move with the velocity $\frac{P}{M}$, leading to an increase in separation of

$$\begin{aligned} \Delta x(p) &= \frac{P}{M} \left(\frac{\partial T}{\partial p_0} \Big|_{P/2} \Delta p \right) \\ &= \frac{2T_m}{\mu} (1 - \alpha)p \end{aligned} \quad (8)$$

Here we have used (4)–(7). Again α appears as the central quantity, determining the sign of Δx .

In [1] the energy spread of the ion source is given as $\frac{\Delta v}{v} < 0.1\%$, which translates into a relative momentum of $p < 4$ a.u. With the parameters of table I the relative error between the linearized ΔT and the correct difference $T(\frac{P}{2} + p) - T(\frac{P}{2} - p)$ is well below $\mathcal{O}(10^{-5})$.

Pedersen *et al* defined a parameter α , too, which we refer to as α_p [5]. From its definition as $\alpha_p = \frac{1}{T} \frac{\partial T}{\partial E_0}$ we calculate with (4)–(7) the following relation:

$$2E_0\alpha_p = \frac{1 - \alpha}{1 + \alpha} \quad (9)$$

It should be noted that $\frac{\partial T}{\partial E_0}$ yields essentially the same information as $\frac{\partial T}{\partial p_0}$ about the sign of the trap's dispersion.

III. TWO NON INTERACTING IONS

Before we look at the coupled motion of two interacting ions, we will study the non interacting case, where we set $W \equiv 0$ in (3). Adding the interaction will then modify this model and the relevant mechanism will become clearer.

Instead of solving the actual equations of motion for the two ions we "take apart" the trap and follow the evolution of the relative coordinate through the three regions of the trap (cf. figure 1): (i) the central field free part, (ii) the mirrors and (iii) the kink region, which connects these two. The evolution of the relative coordinate in each of these parts can then be described by two-by-two mappings of the relative coordinate and momentum. The composite mapping, built up of these building blocks, describes the relevant dynamics.

A. Mapping the free motion

The trap potential $V(x)$ (1) is flat in the central part of the trap and linear in the mirrors; in these regions the Hamiltonian (3) can be separated into CM and relative coordinates.

Without the ions' interaction, the relative momentum p is constant in both the central part and in the mirrors and the distance x evolves freely as

$$x(t) = x(0) + \frac{p}{\mu} t. \quad (10)$$

As the times spent in the mirror and in the central part, T_m and $T_f = \alpha T_m$, are fixed by the CM motion (see equations (4) and (5)), we define two mappings \mathcal{F} and \mathcal{M} that describe this free evolution of the relative coordinate in the central part and in the mirrors, respectively. They differ only in their time duration:

$$\mathcal{F} : \begin{pmatrix} x \\ p \end{pmatrix} \mapsto \begin{pmatrix} x' \\ p' \end{pmatrix} = \begin{pmatrix} x + \frac{\alpha T_m}{\mu} p \\ p \end{pmatrix} \quad (11)$$

$$\mathcal{M} : \begin{pmatrix} x \\ p \end{pmatrix} \mapsto \begin{pmatrix} x' \\ p' \end{pmatrix} = \begin{pmatrix} x + \frac{T_m}{\mu} p \\ p \end{pmatrix} \quad (12)$$

Their interpretation is the following: if the ions have the relative coordinates (x, p) , when the CM enters, e.g., the mirror, these will have evolved to $(x', p') = \mathcal{M}(x, p)$, when the CM leaves this region again.

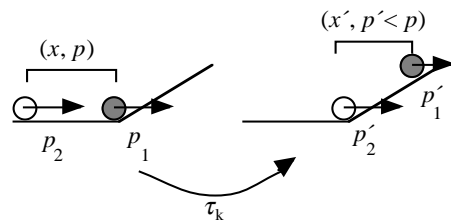


FIG. 2: During the time τ_k , when the two ions are in different parts of the trap potential, they experience a different acceleration due to the mirror potential. Integrating the difference over τ_k results in a compressing change of the relative momentum (13).

B. The momentum kick approximation

For that part of the motion when the two ions are in different parts of the trap potential, the CM and the relative motion are coupled for a time τ_k . This is the time between when the first ion crosses the kink between the flat part and one of the mirrors at $\pm \frac{L}{2}$ and when the second one passes that point (see figure 2). During that time the ions are accelerated relative to each other by the trap potential. For the case of incoming ions, which is depicted in figure 2, this time is:

$$\tau_k = \frac{x}{p_2/m}$$

After this time the momentum p_2 will be the same, $p'_2 = p_2$, but p'_1 has become

$$p'_1 = p_1 + \tau_k \left(-\frac{\partial V}{\partial x_1} \right) = p_1 - \frac{xm}{p_2} F$$

The two ions have nearly the same velocity, so $\frac{p_2}{m}$ is approximated by $\frac{P}{M}$, the velocity of the CM.

If the energy of the two ions of about 4.2 keV differs by 2 eV in the laboratory frame, their momenta will differ by about 1 a.u.: replacing $\frac{p_2}{m}$ by $\frac{P}{M}$ then introduces an error on the order of $\mathcal{O}(10^{-5})$.

The relative momentum $p = \frac{p_1 - p_2}{2}$ now changes as (cf. (4))

$$p' = p - \frac{FM}{2P} x = p - \frac{2\mu}{T_m} x \quad (13)$$

This formula is valid for outgoing ions, too. Through the special geometry of the trap the momentum transfer and the time spent in the mirror are intimately related to each other.

The relative distance x changes, too, but assuming an initial distance of, e.g., $x = 10^7$ a.u., only by a factor of $1 - \mathcal{O}(10^{-3})$; this change of x will be neglected. We also assume that the CM momentum is not affected by this momentum transfer, which is true to the order of $\mathcal{O}(10^{-3})$.

As the ions — in our approximation — do not move relative to each other during τ_k , the motion through the

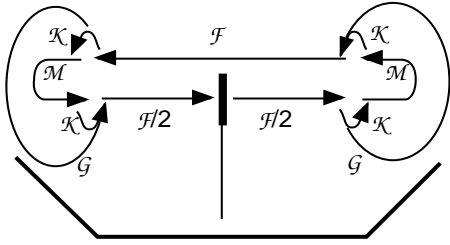


FIG. 3: Sketch of the sequence of mappings during one period of the motion of two non interacting ions (16). The trap is symbolized by the potential and the stylized pickup.

kink region has the effect of an instantaneous momentum "kick" in the relative coordinate, induced by the coupling of the CM and the relative coordinate. This momentum "kick" always pushes the two ions together. We consequently describe the kink by the following mapping \mathcal{K} :

$$\mathcal{K} : \begin{pmatrix} x \\ p \end{pmatrix} \mapsto \begin{pmatrix} x' \\ p' \end{pmatrix} = \begin{pmatrix} x \\ p - \frac{2\mu}{T_m} x \end{pmatrix} \quad (14)$$

C. The composite mapping — the dispersion of the trap

With the mappings \mathcal{F} , \mathcal{M} and \mathcal{K} in hand we are now able to describe the motion of two non interacting ions in the trap. One complete period consists of a sequence of these mappings, cf. figure 3. We start the cycle in the middle of the central region, where in the experiment the pickup is located. The composite map, denoted by \mathcal{P}_{non} , then describes how the observed distance between the two ions changes between successive measurements. It has the following form, with $\mathcal{F}_{\frac{1}{2}}$ describing the free motion for a time $\frac{T_f}{2}$ (cf. (11)):

$$\begin{aligned} \mathcal{P}_{\text{non}} &= \mathcal{F}_{\frac{1}{2}} \otimes \underbrace{\mathcal{K} \otimes \mathcal{M} \otimes \mathcal{K}}_{\mathcal{G}} \otimes \mathcal{F} \otimes \underbrace{\mathcal{K} \otimes \mathcal{M} \otimes \mathcal{K}}_{\mathcal{G}} \otimes \mathcal{F}_{\frac{1}{2}} \quad (15) \\ &= \mathcal{F}_{\frac{1}{2}} \otimes \mathcal{G} \otimes \mathcal{F} \otimes \mathcal{G} \otimes \mathcal{F}_{\frac{1}{2}} \quad (16) \end{aligned}$$

In the second line the effects of the mirror and the two adjacent momentum kicks are combined into the mapping \mathcal{G} . We will later see that the main synchronization process can be understood from this part alone. The composite mapping \mathcal{P}_{non} finally simplifies to

$$\mathcal{P}_{\text{non}} : \begin{pmatrix} x \\ p \end{pmatrix} \mapsto \begin{pmatrix} x' \\ p' \end{pmatrix} = \begin{pmatrix} x - \frac{2T_m}{\mu}(1 - \alpha)p \\ p \end{pmatrix} \quad (17)$$

From energy conservation we know that the momenta p_1 and p_2 , and consequently p , have to be the same, when each of the independent ions has completed the period. The increase in distance, already calculated from the dispersion $\frac{\partial T}{\partial p_0}$ (7) is also reproduced by \mathcal{P}_{non} .

Our mapping model therefore describes the evolution of the relative distance between two independent ions

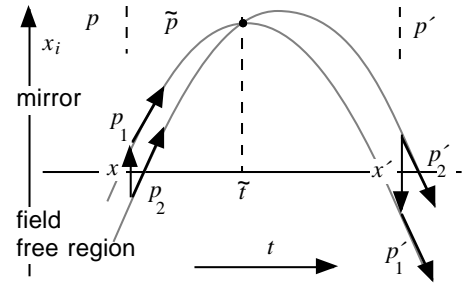


FIG. 4: Sketch of the trajectories of two non interacting ions on their way from the central field free region of the trap through the mirror back into the central part. The horizontal axis is time, the vertical axis denotes the position of the ions in the trap. Ion 2 is here the faster one. The initial relative momentum is p , after the first kick it is denoted by \tilde{p} and after the second kick by p' . The time when the ions' trajectories cross is denoted by \tilde{t} .

with the same accuracy of $\mathcal{O}(10^{-5})$ as the linearized dispersion (7).

D. The mirrors' map: $\mathcal{G} = \mathcal{K} \otimes \mathcal{M} \otimes \mathcal{K}$

Now we will look at the above defined mapping \mathcal{G} (16). From energy conservation and geometrical considerations we see that — without the ions' interaction — the total effect of the mirror is to turn around the direction of the two momenta p_1 and p_2 , and therefore of p (see figure 4):

$$\left. \begin{aligned} p'_1 &= -p_1 \\ p'_2 &= -p_2 \end{aligned} \right\} \Rightarrow p' = \frac{p'_1 - p'_2}{2} = -p \quad (18)$$

The relative momentum changes by $\Delta p = p' - p = -2p$. Each of the two momentum kicks is proportional to the corresponding distance (13), x at the entrance and x' at the exit of the mirror; the intermediate and final momenta, \tilde{p} and p' , are therefore

$$\tilde{p} = p - \frac{2\mu}{T_m} x \quad \text{and} \quad p' = \tilde{p} - \frac{2\mu}{T_m} x' \quad (19)$$

From the above equations (18) and (19) we derive a relation between the distances x and x' and the momentum $p = -p'$:

$$x + x' = \frac{T_m}{\mu} p$$

This relation can also be obtained by evaluating $\mathcal{G} = \mathcal{K} \otimes \mathcal{M} \otimes \mathcal{K}$ directly:

$$\mathcal{G} : \begin{pmatrix} x \\ p \end{pmatrix} \mapsto \begin{pmatrix} x' \\ p' \end{pmatrix} = \begin{pmatrix} -x + \frac{T_m}{\mu} p \\ -p \end{pmatrix} \quad (20)$$

It should be noted that with the experimental parameters of table I, the change of x in the mirror is about

a factor of 10 bigger than Δx after one complete period (8). Most of the mirror's effect, however, is compensated for by the motion in the central part. At $\frac{\partial T}{\partial p_0} = 0$, which corresponds to $\alpha = 1$, both contributions exactly cancel each other.

In figure 4 the time \tilde{t} denotes the crossing of the two ions' trajectories. It is defined by

$$\tilde{x}(\tilde{t}) = x + \frac{\tilde{p}}{\mu} \tilde{t} = 0$$

and evaluates to

$$\tilde{t} = \tilde{t}(x, p) = \frac{T_m \mu x}{2\mu x - T_m p} \quad (21)$$

The limits for $x \rightarrow \pm\infty$ or $p = 0$ are $\tilde{t} = \frac{T_m}{2}$. For finite p and $\frac{x}{p} < 0$, $0 \leq \tilde{t} \leq \frac{T_m}{2}$; for $\frac{x}{p} \geq \frac{T_m}{\mu}$ we have $\frac{T_m}{2} \leq \tilde{t} \leq T_m$. In the intermediate region \tilde{t} is either negative or bigger than T_m , with a singularity at $\frac{T_m p}{2\mu}$. In that case there is no collision inside the mirror, as (21) is only defined in the mirror region.

Equation (21) is meaningful only as long as both ions spend time together in the mirror: if the first ion has already left the mirror when the second one arrives, the above treatment is not valid. This happens when the ions are further away from each other than

$$x_{\max} = T_m \frac{P}{M} = \frac{L}{\alpha} \quad (22)$$

Without interaction the two ions' trajectories cross twice during a given period. This happens either in the mirror or in the central region. The probability w_F for the latter is given by the ratio between the relative distance for which there is no solution of (21) inside the mirror, $\frac{T_m p}{\mu}$, and the distance x_{\max} (22), for which equation (21) is defined. With (5) it evaluates to

$$w_F = \frac{Mp}{\mu P} = \frac{4p}{P} \quad (23)$$

As $p \ll P$, a collision of the two ions in the central part is a highly unlikely event. With the parameters given, w_F is on the order of only $\mathcal{O}(10^{-3})$.

The different possibilities can be visualized by shifting the two (parabolic) trajectories of the ions in figure 4 against each other: as they are plotted in figure 4 we have $0 < \tilde{t} < \frac{T_m}{2}$. This is case (i) of figure 5. If now the trajectory of ion 1 is moved to the right, the crossing time \tilde{t} will slide to the left, until both trajectories intersect at their entrance into the mirror, which means $\tilde{t} = 0$, depicted in case (ii) of figure 5a. When trajectory 1 is shifted further to the right, case (iii), the ions do not cross inside the mirror (cf. the explanation above and equation (23)). The crossing point reappears at $\tilde{t} = T_m$ (iv), i.e., when the ions leave the mirror, and from there it proceeds back in the direction of $\frac{T_m}{2}$ (v). These processes are the framework into which we later incorporate the ions' interaction.

Fig. 5(b) plots the relative momentum $p(t)$ during the course of \mathcal{G} . In all cases the final momentum is $p' = -p$. For cases (i) and (ii) the momentum changes sign only with the second kick, while for cases (iv) and (v) it is reversed already with the first kick. When the crossing takes with $\tilde{t} < \frac{T_m}{2}$ the second kick is the larger one, while if $\tilde{t} > \frac{T_m}{2}$, the first kick is stronger. In all these cases the two kicks have opposite direction.

In the above cases $x(t)$ changes sign in the mirror at $t = \tilde{t}$. In the special case (iii) x does not change its sign and both kicks work in the same direction; here the momentum in the mirror is less than before and after it. In this regime the faster ion enters the mirror first and leaves it second.

It should be emphasized that, without interaction, the relative momentum in the central part of the trap is the same after each period. This is the important conserved quantity. The relative momentum in the mirror, on the other hand, is a measure of the time delay or phase lag of the two ions on their orbit.

IV. ADDING THE ION-ION INTERACTION

We now incorporate the (repulsive) interaction between the two ions into our model. We will see that the repulsive interaction can be modelled as a time delay and we will then introduce this delay into the mappings.

A. The time delay

When both ions are in one of the mirrors or in the central part, the relative coordinate is decoupled from the CM motion (see section III A). The free motion in the relative coordinate is now modified by the interaction $W(x)$ (10). Any collision of the ions is elastic due to the conservative Coulomb interaction. As we are only interested in the final values of x and p , but not in the actual solution of the equations of motion, we adopt a central idea of scattering theory: the whole effect of the ions' collision is described by a phase shift, or, for our treatment, a time delay τ [7]. This delay modifies the propagation time for the freely evolving relative coordinate:

$$x(T) = x(0) + \frac{p}{\mu}(T - \tau) \quad (24)$$

In this ansatz T stands for either T_m or T_f . The time delay τ is clearly a function of the interaction potential and the initial distance and momentum. It can be positive or negative; if the relative motion is delayed we have $\tau > 0$.

B. Modifying the mappings

With the interaction added we now use (24) instead of (10) to map the relative coordinate in the mirrors or the

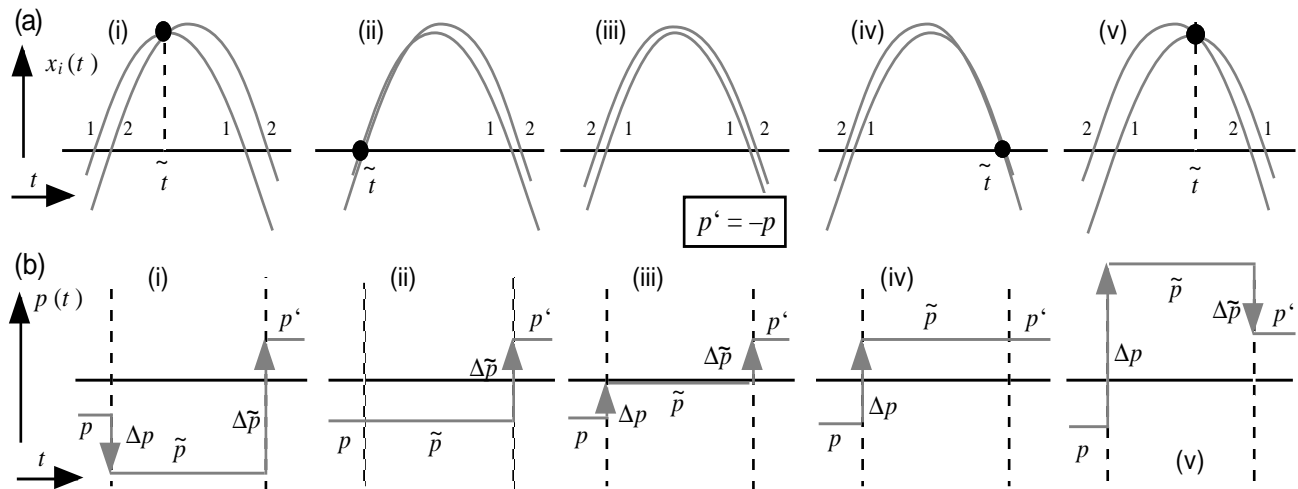


FIG. 5: The different types of trajectories that occur in the mirror region for different initial values; for an explanation please see text.

trap's central part, respectively.

If the initial and final distances are not in the asymptotic region, where $W(x) = 0$, we have to adjust p' , too, to conserve the energy of relative motion. But as our treatment does not depend on a special form of W , we will for the following assume that the collision between the two ions takes much less time than T_m or T_f and that before and after the collision the interaction between the ions can be neglected.

A time delay τ_m in the mirror region may be incorporated directly into (12). It modifies the relative coordinate:

$$\mathcal{M}' : \begin{pmatrix} x \\ p \end{pmatrix} \mapsto \begin{pmatrix} x' \\ p' \end{pmatrix} = \begin{pmatrix} x + \frac{T_m - \tau_m}{\mu} p \\ p \end{pmatrix} \quad (25)$$

The mapping now is a functional of the still unspecified delay $\tau_m = \tau_m(W; x, p)$, which itself depends on the actual form of the interaction potential.

In the non interacting case the mapping in the central part is described by (11). Recall that the ratio of T_f and T_m defines the parameter α , which in turn is related to the dispersion of the trap (7). It will be convenient, therefore, to incorporate a time delay τ_f into a modified α' , defined by:

$$\alpha T_m - \tau_f = \left(\alpha - \frac{\tau_f}{T_m}\right) T_m =: \alpha' T_m \quad (26)$$

The mapping \mathcal{F} is consequently modified to:

$$\mathcal{F}' : \begin{pmatrix} x \\ p \end{pmatrix} \mapsto \begin{pmatrix} x' \\ p' \end{pmatrix} = \begin{pmatrix} x + \frac{\alpha' T_m}{\mu} p \\ p \end{pmatrix} \quad (27)$$

During the short interval of the momentum kick we assume the ions do not move relative to each other (see section III B). Also the trap potential is much stronger than the weak ion-ion interaction. Consequently the mapping \mathcal{K} (14) remains unchanged.

With these modifications the composite mapping for the whole period, starting and ending at the pickup in the center of the trap, becomes a functional of the delays τ_m and τ_f (cf. (16)):

$$\mathcal{P}' = \mathcal{F}'_{\frac{1}{2}} \otimes \mathcal{K} \otimes \mathcal{M}' \otimes \mathcal{K} \otimes \mathcal{F}' \otimes \mathcal{K} \otimes \mathcal{M}' \otimes \mathcal{K} \otimes \mathcal{F}'_{\frac{1}{2}} \quad (28)$$

Here $\mathcal{F}'_{\frac{1}{2}}$ denotes the propagation through only half of the central part, i.e., between the pickup and one of the mirrors: $\mathcal{F}' = \mathcal{F}'_{\frac{1}{2}} \otimes \mathcal{F}'_{\frac{1}{2}}$.

V. LINEAR STABILITY ANALYSIS

Now that we have set up all parts of the model we will quantify the stability of the composite mapping \mathcal{P}' (28) and determine the conditions under which synchronization of the two ions' motion occurs.

We follow the usual lines: the mappings are linearized around the initial values (x, p) by calculating the Jacobi matrix of partial derivatives:

$$J = J(\tau_m, \tau_f) = \begin{pmatrix} \frac{\partial x'}{\partial x} & \frac{\partial p'}{\partial x} \\ \frac{\partial x'}{\partial p} & \frac{\partial p'}{\partial p} \end{pmatrix}.$$

If the eigenvalues λ of J are complex with a length of 1, then the mapping is stable and the ions' motion synchronized; if the λ are real it is unstable and the motion diffusive [8]. According to equations (14), (25) and (27) the eigenvalues are functions of the trap parameters T_m , α and μ and of the time delays τ_m and τ_f .

A. The elementary maps

Through the linearization the time delays become constants. With the constant τ_m and τ_f , and, consequently,

the constant α' , all the maps involved are linear and their Jacobians can be represented by 2×2 matrices. They have the following forms:

$$\mathcal{F}' \Rightarrow \mathbf{F} = \begin{bmatrix} 1 & \frac{\alpha' T_m}{\mu} \\ 0 & 1 \end{bmatrix} \quad (29)$$

$$\mathcal{M}' \Rightarrow \mathbf{M} = \begin{bmatrix} 1 & \frac{T_m - \tau_m}{\mu} \\ 0 & 1 \end{bmatrix} \quad (30)$$

$$\mathcal{K} \Rightarrow \mathbf{K} = \begin{bmatrix} 1 & 0 \\ -\frac{2\mu}{T_m} & 1 \end{bmatrix} \quad (31)$$

The determinant of each of these matrices is equal to 1. Moreover, they all have a double eigenvalue of 1 and a fixpoint at $(x, p) = 0$, independent of the values of T_m , μ , α' and τ_m .

The composite mappings are represented by the corresponding products of the elementary matrices: $\mathbf{G} = \mathbf{KMK}$ and $\mathbf{P} = \mathbf{F}_{\frac{1}{2}} \mathbf{KMKF}_{\frac{1}{2}}$, where $\mathbf{F}_{\frac{1}{2}}$ corresponds to $\mathcal{F}'_{\frac{1}{2}}$ (cf. (28)). Since \mathbf{F} , \mathbf{M} and \mathbf{K} all have a fixed point at $(x, p) = 0$, it follows that \mathbf{G} and \mathbf{P} must as well.

B. Stability of the complete mapping \mathcal{P}

The Jacobian for the complete period can be grouped into the modified mirror $\mathbf{G} = \mathbf{KMK}$ and the field free central region \mathbf{F} : $\mathbf{P} = \mathbf{F}_{\frac{1}{2}} \mathbf{G F G F}_{\frac{1}{2}}$. The stability criterion can, due to this repetitive structure, already be inferred from $\mathbf{P}_{\frac{1}{2}} = \mathbf{F}_{\frac{1}{2}} \mathbf{G F}_{\frac{1}{2}}$. Its explicit form is,

$$\mathbf{P}_{\frac{1}{2}} = \begin{bmatrix} -1 + 2\epsilon(1 - \alpha) & \frac{T_m}{\mu}(1 - \alpha)(1 - \epsilon + \alpha\epsilon) \\ -\frac{4\mu\epsilon}{T_m} & -1 + 2\epsilon(1 - \alpha) \end{bmatrix} \quad (32)$$

where we have defined $\epsilon = \frac{\tau_m}{T_m}$.

The determinant of $\mathbf{P}_{\frac{1}{2}}$ is 1. In section III D we showed that the ions collide *either* in the mirror *or* in the central part; therefore one of the delays vanishes. These two cases correspond to either $\alpha' = \alpha$ or $\tau_m = 0$, respectively. For $\alpha' = \alpha$ and $\tau_m = 0$ the non interacting case is recovered: $\mathbf{P} = \mathbf{P}_{\frac{1}{2}} \mathbf{P}_{\frac{1}{2}} = \mathbf{P}_{\text{non}}$, where \mathbf{P}_{non} is the matrix corresponding to the mapping of equation (17).

1. Collisions in the central part

First we will consider the case of $\tau_m = 0$, i.e., the collisions take place in the central part. As discussed above this case is rare. Then $\mathbf{P} = \mathbf{P}_{\frac{1}{2}} \times \mathbf{P}_{\frac{1}{2}}$ reduces to the dispersion of the non interacting case (17), but with the externally defined α replaced by the modified $\alpha' = \alpha - \frac{\tau_f}{T_m}$. Consequently $\mathbf{P}_{\frac{1}{2}}$ has a double eigenvalue of -1 , i.e., the distance between the ions grows linearly in time according to equation (8) with α replaced by α' .

Which ion is faster is determined by whether α' is bigger or smaller than 1.

As in the non interacting case, the eigenvalues of the composite map for the whole trap are $\lambda_{1/2} = 1$: the ions separate linearly in time, if the modified dispersion is not exactly $\alpha' = 1$.

For $\alpha < 1$, which is the experimentally observed condition for bunching, a negative delay τ_f may bring the trap into the regime where the "effective" dispersion α' becomes 1 and both ions have the same period. Collisions in the central part may therefore synchronize the ions by modifying the dispersion of the trap: their differing momenta remain unchanged, but the distance is, due to the vanishing dispersion, the same every time they pass the trap's center. The possibility of this type of synchronization is small: first collisions in the central part are rare events (see equation (23)) and second, with the eigenvalue of 1 the synchronization, if it occurs, is not stable against perturbations.

2. Collisions in the mirror

In the other, much more frequent case, where the ions collide in the mirrors, i.e., $\alpha' = \alpha$ and $\tau_m \neq 0$, the eigenvalues have the form

$$\lambda_{1/2} = -1 + 2\epsilon(1 - \alpha) \pm 2\sqrt{\epsilon^2(1 - \alpha)^2 - \epsilon(1 - \alpha)}. \quad (33)$$

The unmodified α describes the trap's original dispersion. It is now convenient to define another parameter

$$\gamma = \epsilon(1 - \alpha). \quad (34)$$

Then the eigenvalues (33) simplify to

$$\lambda_{1/2} = -1 + 2\gamma \pm 2\sqrt{\gamma^2 - \gamma}, \quad (35)$$

The argument of the square root, $\gamma^2 - \gamma$, is negative for $0 < \gamma < 1$. In that region the eigenvalues are consequently complex with a length of 1 and they are real for $\gamma < 0$.

The important parameter, as we see, is composed of the time delay τ_m in the mirror and the dispersion of the trap, described by α (7). The sign of this parameter γ determines if the relative motion of the two ions is bounded or not: for $\gamma > 0$, which requires either $\tau_m > 0$ and $\alpha < 1$ or $\tau_m < 0$ and $\alpha > 1$, the eigenvalues λ are complex and the ions' motion is synchronized. For $\gamma < 0$ the eigenvalues are real and the ions separate faster than without interaction. This happens for $\tau_m > 0$ and $\alpha > 1$ or for $\tau_m < 0$ and $\alpha < 1$.

For very small γ , i.e., $\tau_m \ll T_m$ or $\alpha \approx 1$, we can neglect 2γ compared to 1 in (35) and approximate the square root by $\sqrt{\gamma^2 - \gamma} \approx \sqrt{-\gamma}$. The eigenvalues are then of the form

$$\lim_{\gamma \rightarrow 0} \lambda_{1/2} = -1 \pm \sqrt{-\gamma} \quad (36)$$

	$\tau_m > 0$	$\tau_m < 0$
$T_m > T_f$ $\Rightarrow \alpha < 1$	$\gamma > 0$ $\Rightarrow \lambda$ complex synchronization	$\gamma < 0$ $\Rightarrow \lambda$ real diffusion
$T_m < T_f$ $\Rightarrow \alpha > 1$	$\gamma < 0$ $\Rightarrow \lambda$ real diffusion	$\gamma > 0$ $\Rightarrow \lambda$ complex synchronization

TABLE II: Overview of the eigenvalues λ of the composite mapping matrix $\mathbf{P}_{\frac{1}{2}}$ (32) for collisions in the mirror and the corresponding behavior of the ions. For $\gamma = 0$, i.e., $\tau_m = 0$ or $\alpha = 1$, which corresponds to either collisions in the central part or no interaction at all, the eigenvalues are -1 and the ions' separation in phase space grows linearly in time.

Consequently the transition between real and complex eigenvalues is very abrupt and the stability changes completely as the delay or the dispersion changes its sign. Table II gives an overview of the behavior of the eigenvalues for the different values that α and τ_m can take for collisions in the mirror.

The stability analysis is consistent with the experimental observation and the findings of reference [3] that synchronization occurs in the region of $\frac{\partial T}{\partial p_0} > 0$, which in our parametrization corresponds to $\alpha < 1$, or according to [5] to $2E\alpha_p > 0$ (9): to achieve bunching, ions with higher energy must have a longer period. But this criterion alone is not enough; it has to be accompanied by a time delay in the mirror, which in turn requires a repulsive ion–ion interaction.

For the other scenario, where the mapping is stable for $\alpha > 1$, the time delay has to be negative. This is possible if the ions have an attractive potential, e.g., if their charges have opposite signs, but then the electrostatic field of the mirrors could keep only one of the ions trapped; their motion would not even have a chance to synchronize. For two or more equal ions only a repulsive Coulomb interaction is possible; any other interaction like the attractive van der Waals interaction is much weaker and can not compete with the Coulomb repulsion. A negative time delay is also possible when the ions' repulsion becomes comparable to the guiding mirror field: then a repulsion between the ions can lead to a negative delay — the ions “bounce off” each other. But in this case the ions' repulsion would dominate the dynamics and it is questionable if the very weak trap potential would be able to actually trap the ions.

VI. EXPLAINING THE SYNCHRONIZATION MECHANISM

From the stability analysis we identify two different mechanisms that can synchronize the motion of two ions: when the ions collide in the mirror, the relation between the momentum kicks is unbalanced, and when collisions take place in the central part, they modify the effective

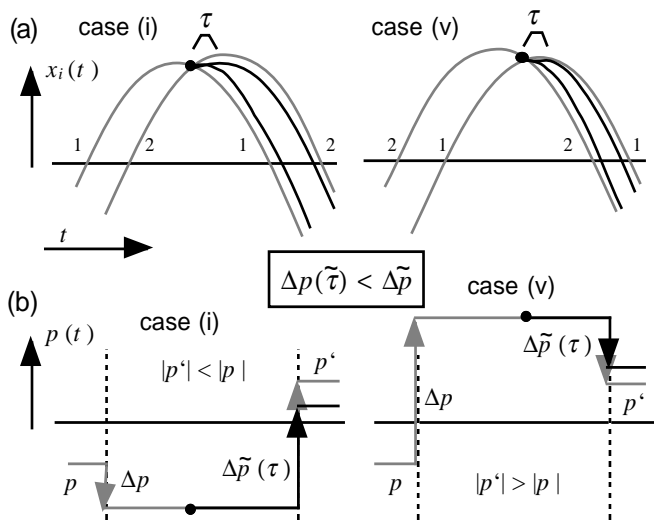


FIG. 6: (a) The ions' positions in the mirror vs. time for case (i), where $\tilde{t} < T_m/2$ and for case (v), where $\tilde{t} > T_m/2$ (cf. figure 5). (b) The corresponding evolution of the relative momentum. A time delay τ_m in the mirror leaves the ions less time to separate after their collision. Consequently the second momentum kick is smaller than without interaction (gray lines).

dispersion. We will now have a closer look at the microscopic dynamics in these two regimes.

A. Collisions in the mirror

To explain how the collisions in the mirror synchronize the ions, it is sufficient to look at the modified mirror map $\mathcal{G}' = \mathcal{K} \otimes \mathcal{M}' \otimes \mathcal{K}$. Without the interaction, \mathcal{G} exactly turns around the relative momentum of the two independent ions: the two momentum kicks add up to $-2p$. During the interval in the mirror the ions approach and re-separate. When the repulsive interaction is added the ions experience a time delay and, consequently, have less time to separate: the second momentum kick (13) will be smaller than without interaction. This is depicted in figure 6. The two sets of trajectories correspond to the configurations (i) and (v) of figure 5, which shows the non interacting case. Now the two kicks, which both are proportional to the corresponding relative distance, will not add up to $-2p$ any more and the relative momentum after the second kick will be either smaller (figure 6, case (i)) or bigger (case (v)) than $-p$, depending on whether the slower or the faster ion enters the mirror first. In either case momentum is effectively transferred from the second onto the first ion, due to the modified coupling between the relative and the CM motion.

If the first ion is the faster one it will gain additional energy through this momentum transfer. Because the period increases with energy, the distance between the two ions will shrink until the slower one overtakes the faster

one. Then momentum is transferred from the faster ion, which is now the second one, onto the slower first one, until the first ion again will be the one with the higher momentum. This process repeats itself over and over, with the ions effectively orbiting around each other in their relative coordinate, stably interlocking and synchronizing their motion.

In the non interacting case the momentum kicks and the time spent in the mirror are intimately related (see (21)). This balance is now offset by the ion–ion interaction. In this way the very small repulsion is amplified to counterbalance the trap’s dispersion and suppress the separation of the ions.

B. Collisions in the central part

When the ions collide in the central part of the trap the mechanism is completely different. As shown in section III D, in this regime the faster ion enters the mirror first and leaves second (see figure 5(iii)). For this mode to be stationary the dynamics has to be symmetric in both mirrors; consequently the ions have to exchange their roles in the collision in the central part of the trap: the first slower ion is accelerated by the faster second, which comes from behind. With this mechanism, which was dubbed “bricking motion” by Zajfman *et al* [9], each of the ions is the faster for one half period and the slower one on the other side of the trap. This way both ions have the same energy, and therefore the same period on average, even for $\alpha \neq 1$.

VII. ILLUSTRATIONS AND EXTENSIONS

In the previous sections we have derived the conditions for stability and explained the underlying mechanism of our mapping model. Now we will check the validity of our description with regard to the two central simplifications — the instantaneous ion–ion interaction and the constant slope of the mirror potentials.

A. Poincaré maps for constant τ_m

In section VI A we explained that in the bunching mode the ions oscillate around each other. This “orbiting” of the ions can be conveniently depicted in a Poincaré section of the repeated mapping \mathcal{P}' (28) by plotting the relative coordinate and momentum after each iteration.

In section V we linearized \mathcal{P}' , which resulted in a constant τ_m . Figure 7 shows the results of the repeated mapping for an arbitrarily chosen $\tau_m = 3 \times 10^8$ a.u.: Panel (a) is calculated for $\alpha = 0.956$ based on the experimental values given in table I, resulting in ellipses.

If we increase α to $1.046 = 1/0.956$ into the unstable regime, with all the other parameters unchanged, the

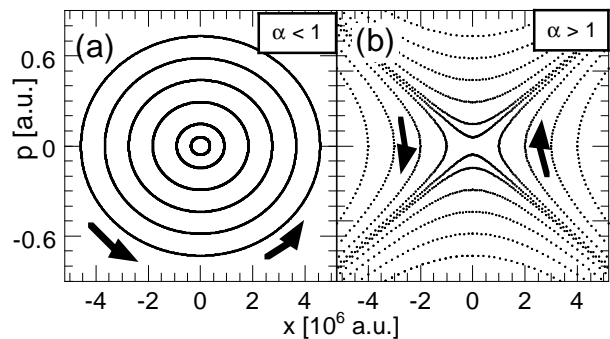


FIG. 7: Poincaré section for the composite mapping \mathcal{P} for a constant $\tau_m = 3 \times 10^8$ a.u. Panel (a) shows the bunching and (b) the diffusive behavior. The arrows denote the direction of the phase space flow.

Poincaré section becomes hyperbolic, see panel (b): the ions separate with a speed that increases with their distance.

Note that the phase space flow in figure 7(a) is in the direction opposite to that of an isolated particle in an external harmonic potential.

For a constant τ_m and $\alpha < 1$, using the linearized mapping $\mathbf{P}_{\frac{1}{2}}$ (32) we can derive a conversion factor between the maximal distance x_{max} and the maximal momentum $p_{max} = \frac{x_{max}}{\beta}$ of a Poincaré ellipse. It evaluates to

$$\beta = \frac{T_m}{2\mu} \sqrt{\frac{1-\alpha}{\epsilon} - (1-\alpha)^2} \quad (37)$$

$$= \frac{T_m}{2\mu\epsilon} \sqrt{\gamma - \gamma^2} \quad (38)$$

The parameter γ (34) is the same as defined in the context of the stability of the bunching mode (cf. section V B 2), but the sign of the argument of the square root is reversed. For the Poincaré sections shown above with $\tau_m = 3 \times 10^8$ a.u. we get $\beta = 7.6 \times 10^6$ a.u.

From equation (37) we see that β decreases when the trap is brought closer to the transition at $\alpha = 1$: the maximal momentum increases until the point that the ellipses “break apart” and become hyperbolas.

B. Trajectory calculations: non instantaneous delay

With the simple mapping model we were able to derive the condition for a stable bunch and to give a microscopic explanation for the coupled motion of the two ions. In order to verify that the discrete description of the relative coordinate implied by the mapping is accurate, we compare our results to trajectory calculations, i.e., to the exact solution of the equations of motion of the two ions from the full Hamiltonian (3).

To allow the ions to pass by each other in our one dimensional model we replace the Coulomb repulsion $\frac{1}{|x|}$

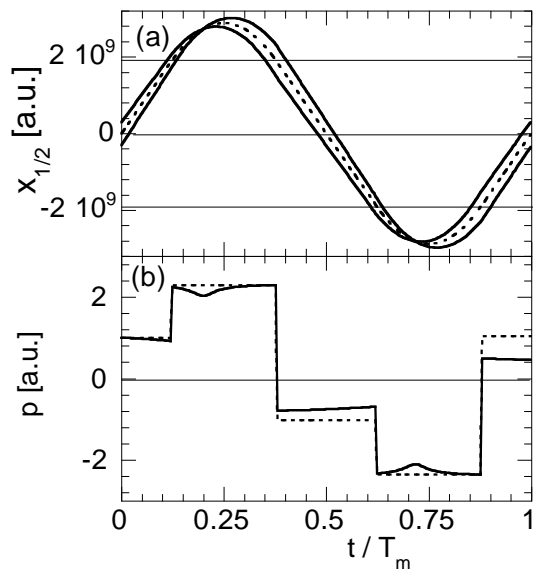


FIG. 8: Solution of the equations of motion for two ions for one period T with and without interaction. These plots should be compared to the results of the mapping (figure 6). Panel (a) plots the positions: the distance of the two ions (—) from the CM's trajectory (---) is multiplied by a factor of 300. The horizontal lines at $x_{1/2} = \pm 1.89 \times 10^9$ a.u. denote the beginning of the mirror regions. (b) shows the relative momentum between the ions with (—) and without (---) the interaction. The temporary slowing down due to the interaction is clearly visible.

between the ions by a so called "softcore Coulomb interaction" [10]:

$$W(x) = \frac{1}{\sqrt{x^2 + d^2}}$$

The "softcore parameter" or "impact parameter" d is a measure of how close the two ions have to come when passing each other; it describes the diameter of the ion beam in the trap potential. For the trajectory calculation we set this value to $d = 10 \mu\text{m}$. This value is much smaller than the real beam, but still the ions' interaction is weaker than the trap potential by about four orders of magnitude.

Figure 8 we show the result of a trajectory calculation for one period T (6) for the initial values $x = -10^6$ a.u. and $p = 1$ a.u. All other parameters were set to the experiment's values of table I, resulting in $\alpha = 0.956$. Panel (a) shows the CM's position vs. time as a broken curve and the two ions' coordinates. Their distance from the CM has been increased by a factor of 300 for clarification. Case(i) of figure 6(a) is reproduced during the time interval $0.1T < t < 0.4T$ and, symmetrically in the other mirror, during $0.6T < t < 0.9T$. Panel (b) compares the relative momentum with (solid line) and without (broken line) interaction: the "discontinuities" of the momentum kicks are clearly seen, cf. figure 6. Without interaction the momentum is reversed after each mirror and returns to its initial value: $p'' = -p' = p$ after one full period.

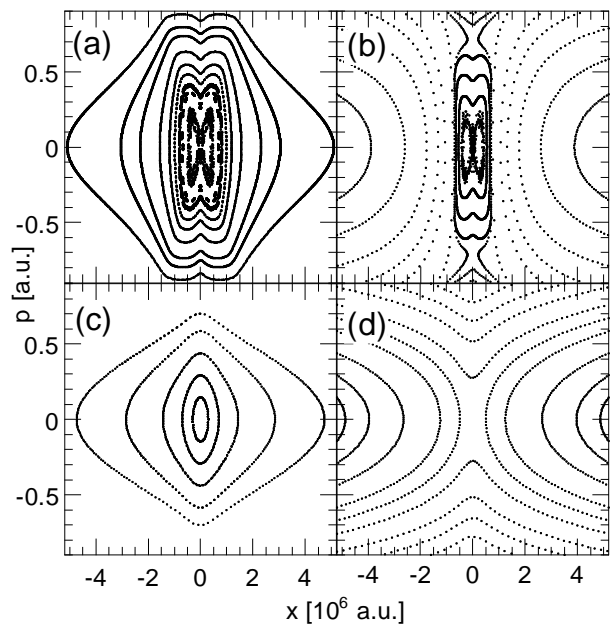


FIG. 9: Poincaré sections from trajectory calculations for the stable regime of $\alpha = 0.956$ (a) and for the unstable regime with $\alpha = 1.046$ (b). The lower row is the result of the repeated mapping \mathcal{P} with a non constant τ_m from (39) for the same values of α as (a) and (b): (c) shows the stable and (d) the unstable regime.

The main difference between the trajectory calculations and the mapping description is that in our mapping approach the ions' collisions are instantaneous and confined to the mirror. In the trajectory calculations the ion-ion interaction takes place anywhere in the trap on a time scale comparable to T_m for small relative momenta. This can be seen in figure 8(b) where the relative momentum deviates visibly from the non interacting case for about half of the time spent in the mirror.

The trajectory shown in figure 8 confirms that the processes of figures 5 and 6, which we used to explain the mechanism, exist. In order to confirm both the bunching condition and the dominance of the collisions in the mirror, we created Poincaré sections from the trajectory calculation, too. The stability of the synchronization shows up in the overall elliptic or hyperbolic structure of the orbits. If the ions are synchronized dominantly through delaying collisions in the mirror, as we propose, the orbits will be (deformed) ellipses, whereas the alternating "bricking motion" (cf. section VI B) will lead to a discrete structure.

The Poincaré sections from the trajectory calculation are shown in figure 9 in panels (a) and (b). In the stable regime, i.e., for $\alpha < 1$, shown in (a), the orbits are deformed ellipses: the ions orbit around each other. The strength of the interaction, and therefore the local curvature of the orbit, varies with the relative distance and the momentum, but it can still be summarized by a time delay.

Only for small distances and momenta does the structure of the Poincaré section become more complicated: the fixpoint at $(x, p) = 0$ is surrounded by a chaotic layer. When the ions are very close together the effective delay changes so much between successive collisions that the quasicontinuous orbits are broken up and consecutive points are distributed randomly in the central region of the Poincaré section.

The agreement between the Poincaré sections from the mapping and from the trajectory calculations can be improved, when the constant τ_m of figure 7 is replaced by a momentum dependent delay. That the delay depends only on the relative momentum is motivated by our ansatz that the ions reach the asymptotic region again after the collisions. Then the delay does not depend upon the initial and final distance, but only on the speed with which the ions pass each other. In figure 9(c) we show the result of the mapping with the ansatz

$$\tau_m = \tau_m(p) = \frac{C}{\sqrt{|p/p_0|^3 + 1}}. \quad (39)$$

The functional form and the parameters — $C = 3 \times 10^9$ a.u. and $p_0 = 1$ a.u. — were chosen to give orbits of a comparable structure and size as the trajectory calculations of panel (a).

In figure 9(b) we increased α into the unstable regime to $\alpha = 1.046$. Then the trajectory calculation becomes unstable, just as the mapping, except for a small island around $(x, p) = 0$. Even this island vanishes when α is increased further. The stability condition is $\alpha < 1$ as in the mapping, but the transition is less abrupt than with the mapping approach.

Panel (d) plots the corresponding Poincaré section of the mapping with the momentum dependent delay of equation (39). Again, as was the case with panels (a) and (c) in the bunching regime, the overall structure is comparable to the trajectory calculation of (b). The small stable island does not exist, though.

The Poincaré surfaces of section provide a further indication that the mapping ansatz is an excellent representation of the full trajectory dynamics with respect to both the dominant synchronization mechanism and the stability condition.

C. Non-linear mirror fields

Above, we modelled the trap with a constant gradient mirror field (1). This allowed us to decouple the relative coordinate from the CM motion. We now have to ensure that our results and explanations are also valid when the mirror field is not linear in the experiment.

Two conditions must be fulfilled for synchronization to occur in our model (cf. sections VB 2 and VIA): (i) the total dispersion $\frac{\partial T}{\partial p_0}$ of the trap has to be positive and (ii) the interaction has to delay the ions in the mirror, so that the relative momentum is not exactly reversed.

It is easy to see that the overall positive dispersion is not restricted to constant mirror field configurations; any mirror field that increases slower than harmonic will do. The mirror only has to be “long” enough so that it can compensate the negative dispersion of the field free part of the trap.

If the mirror potential is not linear it nevertheless reflects the individual momenta of two non interacting ions. The relative and the CM motion can not be separated any more, but the evolution of the relative coordinate — and consequently the momentum reflection — can be described by an alternation of infinitesimally small kicks and free evolutions.

The ions’ interaction is then added into this succession of mappings as a set of infinitesimal delays, each modifying the balance between the adjacent kicks. The overall effect is the same as with the linear slope: when the ions repel each other they leave the mirror with a smaller distance and the second ion transfers energy onto the first.

Consequently the conditions for synchronization and the explanations given remain unchanged for an arbitrary mirror field.

D. Connection to previous explanations

The approach presented here has several aspects in common with the one recently given by Strasser *et al* [3]. In fact the propagation matrices for the non interacting ions are identical. In the Strasser model the composite mapping (17) derived from these matrices is cast into an effective reduced mass m^* (see equations (6) and (8) of reference [3]). When the ions repel each other, m^* has to be negative for the relative motion to be bound. This leads to the bunching condition of a positive dispersion of the trap, i.e., $\frac{\partial T}{\partial p_0} > 0$. Both the trap’s dispersion and the ions’ repulsion are described in a mean field ansatz; the Strasser model is therefore very robust with respect to the exact form of the trap potential or the details of the ions’ interaction, but can not give an explanation of the underlying microscopic dynamics.

Both the Strasser and our model require $\alpha < 1$ for bunching, but whereas in our approach *any* delay $\tau_m > 0$ is sufficient to couple the ions, the Strasser model requires a minimum density in the bunch, i.e., a minimum interaction strength, because it confines the test ion to stay inside the bunch.

By comparing equation (10) of reference [3] with our equation (32) we can relate the static bunch’s parameters to an effective time delay $\tilde{\tau}_m$:

$$\tilde{\tau}_m = \frac{Nq^2T_m^3}{16\pi m\epsilon_0R_0^3}(1 - \alpha) \quad (40)$$

The bunch consists of N ions of charge q and mass m and has a radius R_0 ; ϵ_0 is the dielectric constant.

From the phase space flow of the Poincaré sections we see that in the diffusive regime the faster ions pass the

pickup in the front of the bunch. This was already observed in [5]. In the bunching regime, though, this ordering is not simply inverted. The Poincaré sections are symmetric with respect to the coordinate and the momentum axis, consequently each of the ions is on average in front for half of the time and has the higher momentum for half of the time, when the CM passes the pickup.

VIII. SUMMARY AND CONCLUSIONS

In this paper we have set up a model to describe the motion of two ions in an "ion trap resonator", an ion trap, which essentially consists of two spatially separated electrostatic mirrors. Our one dimensional model describes the evolution of the ions' relative coordinate and momentum with three simple mappings: one, each, for the free evolution in the central field free region of the trap and in the mirrors, while the third mapping describes the connecting kink between these regions: here the relative coordinate is coupled to the center of mass motion. The coupling gives rise to an instantaneous compressing kick in the relative momentum. The interaction between the two ions is summarized by a time delay, which shortens or lengthens the time for the free evolution either in the mirror or in the central part.

The three mappings allow us to perform a linear stability analysis of the composite mapping for the whole trap. Without delay, i.e., without interaction, the mapping model reproduces the behavior of two independent ions; with the delay added we identify the criteria for the stable synchronized motion: the trap has to be operated in a regime where the period of the ions in the trap increases with their energy *and* the ions have to be delayed by their repulsive interaction, when they cross their paths in the mirror. This confirms the experimental findings that the dispersion of the trap has to be positive.

Based on these simple building blocks we are able to

describe, how the interaction modifies and couples the motion of the two ions in the bunching regime: without the interaction ions with different energies separate linearly in time due to their different periods in the trap. A time delay in the mirror, which describes the repulsive interaction, now modifies the balance of the coupling between the relative and the CM motion at the kink, so that during each pass through the mirror momentum is transferred from the second onto the first ion. This additional energy increases the first ion's period and lets it fall back against the other one until they have exchanged their places. Now the energy is shuffled back onto the other ion, until they exchange their position again and the circle is completed: in the stable region the ions oscillate around each other, constantly transferring energy back and forth between them.

Trajectory calculations confirmed that the ions are synchronized dominantly by the microscopic process of collisions in the mirror that we had derived from the mappings together with an instantaneous interaction. This continuous description reproduces the stability conditions, too. We also verified that our model is valid for arbitrary forms of the mirror potential.

Our model of two ions can also be applied to the dynamics of a test ion inside a bunch. The microscopic picture of the ions' motion, which was developed in this paper, then allows us to identify the important regions of the trap and to explain how they shape the bunch. This will be the subject of a forthcoming publication [6].

Acknowledgments

We thank Daniel Strasser and Daniel Zajfman for constructive discussions and further explanations of the experiment.

This research was funded by the Israel Science Foundation.

-
- [1] H B Pedersen *etal*, *Phys. Rev. Lett.* **87** (2001) 055001
 - [2] A G Marshall, C L Hendrickson and G S Jackson, *Mass. Spec. Rev.* **17** (1998) 1
 - [3] D Strasser *etal*, *Phys. Rev. Lett.*, accepted
 - [4] H B Pedersen *etal*, *Phys. Rev. A* **65** (2002) 042703
 - [5] H B Pedersen *etal*, *Phys. Rev. A* **65** (2002) 042704
 - [6] T Geyer and D J Tannor, to be published
 - [7] J R Taylor, "*Scattering Theory*", John Wiley & Sons, 1972
 - [8] see, e.g., I Percival and D Richards, "*Introduction to Dynamics*", Cambridge University Press, Cambridge, 1982
 - [9] D Strasser, private communication
 - [10] R Grobe, J H Eberly, *Phys. Rev. A* **48** (1993) 4664